Journal Name

RSCPublishing

ARTICLE

Time-resolved photoelectron imaging of the isolated deprotonated nucleotides

Cite this: DOI: 10.1039/xoxxoooooox

Adam S. Chatterley,[†ab] Christopher W. West[a], Vasilios G. Stavros[b] and Jan R. R. Verlet*[a]

Received ooth January 2012,
Accepted ooth January 2012

DOI: 10.1039/xoxxoooooox

www.rsc.org/

Using time-resolved photoelectron spectroscopy, the excited state dynamics of gas-phase mass-selected nucleotide anions have been monitored following UV excitation at 4.66 eV. The spectra reveal that the dynamics of the 2'-deoxyguanosine 5'-monophosphate anion ($dGMP^-$) are very similar to those of the adenosine nucleotide ($dAMP^-$) and insensitive to a solvation environment. Comparison of our results with other literature suggests that nucleotides of the two purine bases share a common relaxation pathway, whereby the initially populated $^1\pi\pi^*$ states relax to the ground electronic state without involvement of any other intermediary electronic states. In the analogous pyrimidine nucleotides of thymine and cytosine, $dTMP^-$ and $dCMP^-$, no such unified mechanism is observed. Photoexcited $dTMP^-$ behaves much like the isolated nucleobase thymine, exhibiting rapid relaxation to the ground electronic state, although with a minor long-lived channel. On the other hand, isolated $dCMP^-$ is longer lived than its cytosine nucleobase, and hence it appears that the presence of the sugar and phosphate in the nucleotide arrangement leads to a modification of the available relaxation pathways. Nucleotides are the basic monomer building blocks of DNA and our results present important new benchmark data to develop an understanding of the molecular mechanism by which photodamage can be mediated when DNA is exposed to UV light.

Introduction

The photophysics of DNA are a subject of great interest, as ultraviolet (UV) light is capable of inducing harmful strand breaks and mutations.[1-3] Despite the constant irradiation from solar light, photoinduced mutations are rare, and thus it appears that nature has selected the structure of DNA to have in-built photoprotective mechanisms. Part of this photoprotection takes the form of ultrafast non-radiative relaxation processes which enable potentially damaging electronic energy to be rapidly dispersed as harmless thermal energy. A major goal in the photochemistry and photobiology communities has been to develop a molecular level understand of these relaxation mechanisms.

The UV absorption spectrum of DNA is dominated by the excitation of the four nucleobases: adenine (Ade), guanine (Gua), thymine (Thy) and cytosine (Cyt). These are aromatic species and possess a strong UV absorption around 4.7 eV (264 nm).[4] In all four nucleobases, this UV absorption populates a $^1\pi\pi^*$ excited state and considerable efforts have been devoted to understanding the photophysics of the isolated (gas phase) nucleobases and related chromophores. All the nucleobases possess decay mechanisms that lead to rapid relaxation to the ground electronic state. In the purine nucleobases (Ade and Gua), this relaxation occurs on a < 1 ps timescale, whilst in the pyrimidine nucleobases (Thy and Cyt) relaxation is somewhat slower, though still < 10 ps. A combination of experimental and theoretical work has provided great insights towards determining the plausible mechanisms by which excited state flux undergoes relaxation; in all cases the relaxation proceeds non-adiabatically by exploiting conical intersections (CIs) where an electronically excited state intersects the ground or an intermediate excited state.[1-3]

Although gas phase studies have been extremely important in deciphering the photophysics of isolated nucleobases,[5-13] this reductionist approach has been limited due to the involatility of larger DNA components. In biological systems, DNA is a polymer of nucleotides, each composed of a nucleobase bound to a deoxyribose molecule and a phosphate group (see Fig. 1 for a representative example). To progress, the major question is: to what extent are the relaxation mechanisms in isolated nucleobases still active in their nucleotides, oligonucleotides and ultimately DNA? Solution phase studies have gone a long way to answering these questions, as transient absorption and

fluorescence upconversion experiments can easily be compared between single nucleobases and nucleotides or oligonucleotides.[14-20] These results have shown that, to a first approximation, the relaxation mechanisms of solvated nucleobases and nucleobases within nucleotides are very similar. On the other hand, interactions between stacked nucleobases within a DNA strand can lead to the formation of excimer states, which may result in remarkably different relaxation dynamics.[21-25] However, even in these large systems, internal conversion to the ground state remains a dominant decay route. In general, mechanistic assignment of solution phase data is complicated by selection rules and solvent broadening, and additionally it is a much more challenging environment for computational chemistry to simulate than the gas phase. In the gas-phase, these solvent-induced complications are not present, but to date, have been limited in size to the study of Cyt, Ade and Thy.

We have recently demonstrated how a combination of electrospray ionization (ESI) and time resolved photoelectron spectroscopy (TRPES) could be used to build up complexity and size from an isolated nucleobase towards DNA. We demonstrated this using the (deprotonated) nucleotide of adenine, 2'-deoxyadenosine 5'-monophosphate (dAMP$^-$, see Fig. 1).[26] Using ESI, transportation of deprotonated nucleotides to the gas phase is facile, and TRPES provides rich details of the path electronically excited state population takes as the nucleotides decay back to the ground electronic state. Deprotonation occurs on the phosphate group of the nucleotides; hence, the excess charge also resides at this moiety.[27] In the dAMP$^-$ experiments, and those presented herein, a femtosecond UV pulse at 4.66 eV (266 nm) prepares an electronically excited state on the mass selected nucleotide anions, and a second, time delayed, femtosecond pulse at 3.10 eV (400 nm) detaches an electron. Fig. 1 outlines the electronic states involved in these experiments. The kinetic energy of the electron, *eKE*, is analysed using velocity map imaging (VMI). A key feature of this experimental scheme is that, although in principle the total photon energy (7.76 eV) is sufficient to detach the electron from many parts of the anion, including the charge carrying phosphate group, by exploiting the $^1\pi\pi^* \leftarrow S_0$ resonance, we can selectively detach electrons only from the nucleobase moiety.[28] This allows us to think of the experiment as photoelectron spectroscopy on a neutral subgroup, whilst the charged phosphate group remains a spectator.

In our previous dAMP$^-$ experiments, we found that the excited state dynamics of the nucleotide could be modelled using biexponential kinetics. Using a global fitting technique, the energetic components of these two pathways could be deconvoluted, and there was clear evidence of a rapid (< 60 fs) initial relaxation within the initially populated $^1\pi\pi^*$ state, followed by a slower (290 fs) relaxation to the ground electronic state. These results compared extremely well to similar experiments performed on isolated 9-methyladenine (Ade-9Me; methylation occurs on the N atom where the deoxyribose group would attach).[5, 6, 29] Theoretical studies have posited two plausible relaxation mechanisms for dAMP$^-$ and

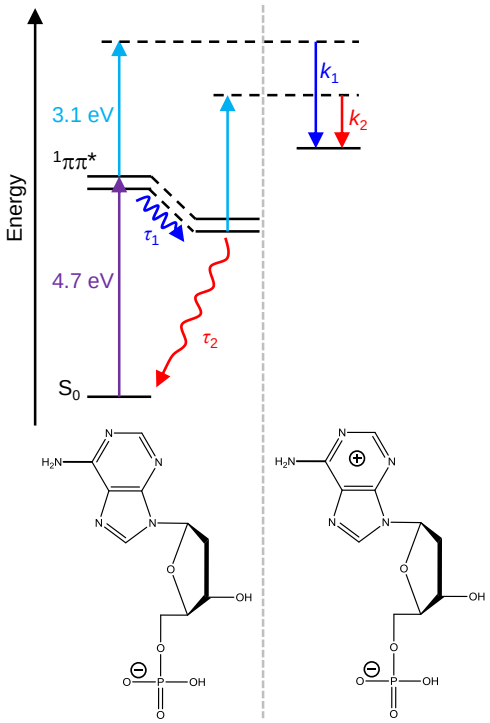

Fig. 1 The pump-probe scheme employed in the experiments, along with a schematic for the relaxation process observed in dAMP$^-$. A 4.66 eV photon prepares the molecule in the $^1\pi\pi^*$ excited state, which subsequently relaxes on this excited state before converting back to the ground state (S_0). Below, the geometry of dAMP$^-$ and the subsequent neutral are shown.

Ade-9Me following excitation to the optically brightest $^1\pi\pi^*$ state (the ^1L_a state).[30-41] Firstly, a two-state mechanism may be active whereby the $^1\pi\pi^*$ state initially converts to a lower lying $^1n\pi^*$ state, and this then relaxes to the ground state through a CI (termed $^1S_6$ in the Boeyens classification scheme).[42] Alternatively, the relaxation may occur solely on the $^1\pi\pi^*$ state, where first rapid wavepacket motion occurs on this state, followed by internal conversion to the ground state through a CI (termed ^2E). Through comparisons with both Ade-9Me and solution phase dAMP$^-$ data, we concluded that the single-state mechanism was more likely to be operative in gas phase dAMP$^-$.[26] This mechanism is sketched in Fig. 1.

Here, we apply this experimental technique to study the remaining deprotonated deoxynucleotides, 2'-deoxyguanosine 5'-monophosphate (dGMP$^-$), 2'-deoxythymidine 5'-monophosphate (dTMP$^-$), and 2'-deoxycytidine 5'-monophosphate (dCMP$^-$). The purine base within dGMP$^-$ is especially interesting as no TRPES has ever been performed on isolated Gua, due to its low volatility,[43] so it is much less well understood than Ade derivatives. dTMP$^-$ and dCMP$^-$ contain the pyrimidine nucleobases, which follow different mechanisms from the purine bases, but appear to follow the same general theme. We show that dGMP$^-$ behaves in a similar manner to dAMP$^-$, and likely shares a very similar excited state relaxation pathway. dTMP$^-$ shows similar dynamics to isolated thymine, and hence very likely follows a similar relaxation route. Finally dCMP$^-$ is shown to behave rather differently from isolated Cyt,

suggesting that the addition of the sugar/phosphate backbone significantly alters the dynamics of this nucleobase.

Experimental

The experiment has previously been described in detail,[44-46] and only a brief overview shall be presented here. Isolated nucleotides were produced using ESI at –2.5 kV with ~ 1mM solutions of the sodium salts of the nucleotides (Sigma-Aldrich, >99% purity) in methanol. Anions were accumulated in ring electrode trap, where they are thermalized to ~300 K, and then ejected into a collinear time-of-flight mass spectrometer at a 50 Hz repetition rate. Mass selected ions were intersected by femtosecond pump (4.66 eV, 266 nm) and probe (3.10 eV, 400 nm) laser pulses in a perpendicular velocity map imaging arrangement.[47] Detached electrons were imaged using a position sensitive detector. Around 5×10^4 laser shots were accumulated for each pump-probe time delay (t). The 4.66 eV light creates additional background counts, so for each delay an equal number of photoelectron images were accumulated without ions, so that this background could be subtracted. Likewise, to remove one-colour signal produced from the pump pulse, the photoelectron image at a delay of –1 ps (probe pulse precedes pump pulse) was subtracted from all images. Images were deconvoluted using the polar onion peeling algorithm[48] to derive the photoelectron spectra and photoelectron angular distributions. The latter reveal no time-resolved dynamics and will not be discussed further. The spectrometer was calibrated using the known spectrum of iodide, and has a resolution $\Delta eKE/eKE \approx 5\%$.

Femtosecond laser pulses were derived from a commercial Ti:Sapphire oscillator and regenerative amplifier, delivering fundamental pulses centred at 1.55 eV (800 nm) and with ~ 50 fs duration. The 4.66 eV pump pulse was produced using a combination of second harmonic and sum frequency generation with the fundamental, in a series of two type I β-barium borate (BBO) crystals. The 3.10 eV probe pulse was produced by second harmonic generation in a further type I BBO crystal. The two pulses were delayed relative to each other using a motorized delay line. Both pulses were combined collinearly using a dichroic mirror, and were loosely focused into the interaction region using a curved metal mirror. The intensity of both beams were below 10^{11} W cm^{-2}. The cross-correlation of the two beams was estimated by fitting the rising edge of the data to be approximately 120 fs, providing a temporal resolution of ~60 fs.

Analysis

All three nucleotides were analysed using a global fitting routine, in an identical manner to previous TRPES studies on nucleobases,[5] and our recent work on the dAMP$^-$ nucleotide.[26] Global fitting operates by fitting spectra at all time delays simultaneously to the same set of time constants for a sum of i exponential decays:

$$S(eKE,t) = \sum_i G(t) * k_i(eKE) e^{\frac{-(t-t_0)}{\tau_i}}$$

where $k_i(eKE)$ is the decay associated spectrum (DAS) corresponding to the exponential decay with a time constant of τ_i. t_0 gives the temporal position of overlap between pump and probe pulses, and $G(t)$ is the Gaussian instrument response function (120 fs). The Levenberg-Marquardt algorithm (implemented in the Matlab optimization toolbox) is used to minimize the sum of the squares of the difference between $S(eKE,t)$ and the experimental dataset.

The shapes of the DAS are highly informative in guiding the interpretation of the spectra. In particular, any negative component corresponds to an exponential rise in that energy region, concomitant with a decay in the positive regions. This can be interpreted as a flow of population from the positive region into the negative, which may be observed due to either a change in electronic state, or relaxation within a single electronically excited state.[49] It is important to note that global fitting *cannot* precisely capture large amplitude motions in the time resolved photoelectron spectrum; if motion of population occurs which does not behave as one state decaying into another, then the fitting algorithm is only able to approximate this motion.[50] In instances where the motion is relatively fast compared to the instrument response function, however, the global fitting approximation is valid.

In all the photoelectron spectra and DAS presented, there is a small amplitude of signal with an *eKE* that extends beyond the maximum energy expected from just the pump (4.66 eV) and probe (3.10 eV) photons. This signal can be attributed to two-photon probing of the system, giving a combined probe energy of 6.20 eV. The two-photon signal is most prominent in the dTMP$^-$ data, although it is visible in the other nucleotides also. The two-photon spectra resemble the one-photon spectra observed at lower *eKE*, but blue shifted by 3.10 eV. In principle, the presence of the two-photon peak extends the probing range significantly, although its weak intensity makes concrete assignments difficult. The ability to significantly extend the probe window is noteworthy in that it allows the adiabatic onset of photoelectron signal to be observed, and hence the Franck-Condon detection window. In the DAS, the same dynamics are assigned to the two-photon probe signal as the one-photon probe signal, indicating that we are capturing all the dynamics of the system, and there are no further processes lying energetically below the one-photon probe limit.

Results and Discussion

dGMP$^-$

Studying the dynamics of the isolated purine nucleobase Gua presents a particular challenge, given that Gua tends to undergo thermal decomposition upon heating in a molecular beam apparatus.[43, 51] As such, gas phase experiments on Gua are especially cumbersome. Additionally, Gua can form multiple

stable conformers in the gas phase,[52-54] that further complicates experiments. Time resolved ion yield (TR-IY) experiments with mass selective product detection (which are sensitive only to the product of interest) are the only reported excited state dynamics experiments on isolated Gua.[9, 10] Photoexcitation at 4.7 eV, resulted in biexponential kinetics, with lifetimes of 148 fs and 360 fs for the two components.[9]

Gua has, however, been the focus of several *ab initio* calculations. These reveal that, at the ground state equilibrium geometry, the S_1 state is the ^1L_a ($^1\pi\pi^*$) state. At higher energy lie the $^1n\pi^*$ and ^1L_b ($^1\pi\pi^*$) states, which are close in energy.[55-63] Calculations of CIs reveal a similar pattern to Ade: three CIs have been located which may be active in the relaxation of Gua.[3, 57, 59, 60, 62, 64] The first two have a geometry puckered at the C^2 position (see Fig. 2a for atom label scheme), analogous to the ^2E CI in Ade. Both of these CIs, which differ only in the geometry of the amino moiety, are between the ^1L_a and S_0 states. The third CI has a geometry with a C^6 pucker, again like in Ade, and this CI is associated with a state of mixed $^1n\pi^*$ and $^1\pi\pi^*$ character. There are also $^1\pi\sigma^*$ states associated with the N^1-H and $N^{(amino)}$-H bonds, which possess CIs that intersect the ground state,[60] although most recent theory does not consider these states. Minimum energy path calculations suggested that the rapid decay observed was attributed to direct decay from the ^1L_a state through the ^2E CIs,[59] and the longer lived component was attributed to dynamics via the $^1n\pi^*/^1L_b$ mixed state. More recently, nonadiabatic dynamics simulations have been performed which indicate that dynamics occur almost exclusively on the first $^1\pi\pi^*$ state, with almost all population relaxing through the two ^2E CIs,[62] although an earlier simulation suggested that the C^6 pucker CI may also be involved.[65]

In the solution phase, Gua itself is rarely studied as it has poor solubility, although $dGMP^-$ has been studied in a number of experiments with transient absorption[1, 16, 66] and fluorescence upconversion.[14, 16, 19, 67 14, 16, 19, 64] As for gas phase Gua excited at around 4.7 eV, solvated $dGMP^-$ is observed to relax through biexponential kinetics.[1] Recent measurements give the short lifetime, $\tau_1 = 120$ fs and the longer lifetime, $\tau_2 = 680$ fs.[16] Computational studies show that solvation dramatically blue-shifts the first $^1n\pi^*$ state, to the extent where it is considered to be unlikely to have any substantial influence on the dynamics.[65, 68] Instead, *ab initio* results have proposed that all dynamics occur upon the ^1L_a state, and any population on the ^1L_b state converts to the ^1L_a in < 20 fs.[68] The dynamics then proceed purely through CIs between the ^1L_a and S_0 states, although there are indications that the presence of the solvent influences which path – and ultimately which CI – is accessed to relax back to the ground electronic state.

The combination of ESI and photoelectron imaging allows us, for the first time, the record the time resolved photoelectron spectrum of a Gua moiety in the gas phase (albeit in its nucleotide). Background subtracted time resolved photoelectron spectra on the $dGMP^-$ nucleotide are presented as an intensity plot in Fig. 2b. Immediately following excitation, a feature is seen extending to ~3 eV, which rapidly decays in < 200 fs. At

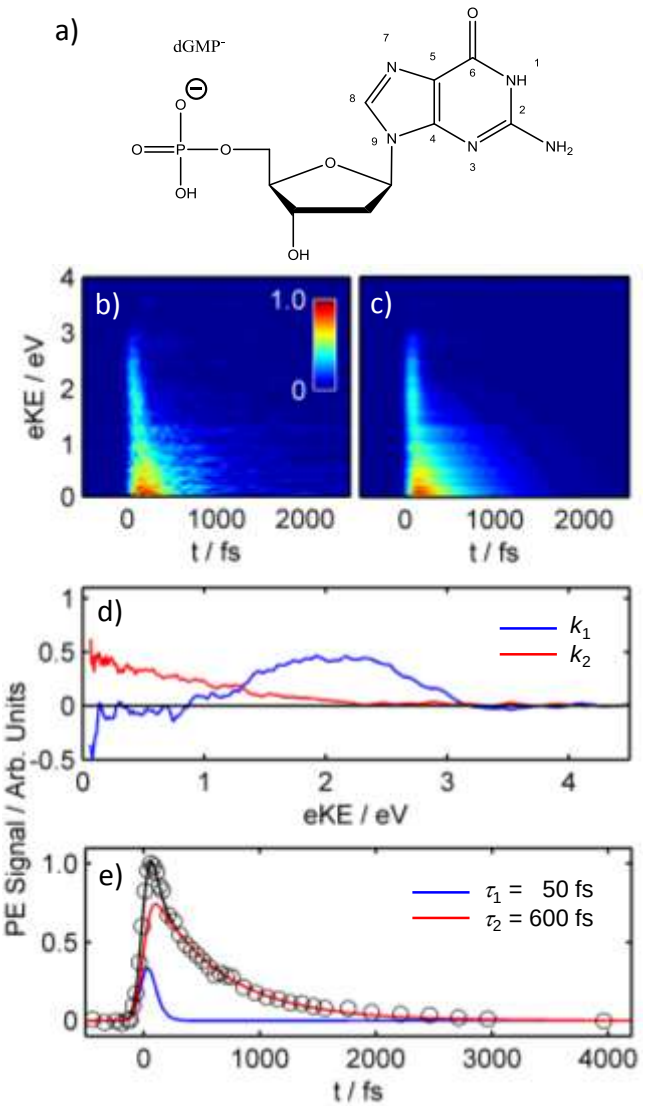

Fig. 2 a) Structure of $dGMP^-$; b) TRPES data from $dGMP^-$, presented as a false-colour plot; c) global fit to the TRPES data, using two exponential decay functions; d) decay associated spectra showing the spectra of the two fit components used to produce the fit; and e) integrated photoelectron signal as a function of delay time. Open circles give experimental data, coloured lines give the two exponential decay functions, and black line gives the total fitted integral.

lower *eKE*, a second feature is observed, which has a slightly delayed onset compared to the higher *eKE* feature (see Fig. S3 in the supporting information). This lower energy feature decays on a much slower timescale, taking ~1000 fs to substantially decay. The total integrated electron signal is shown as a function of delay time in Fig. 2e; the biexponential decay kinetics are readily visible.

The global fitting algorithm disentangles the spectra of the two decay components, and provides quantitative lifetimes. Fig. 2c shows the intensity plot of a global fit to the $dGMP^-$ data, using two decay components. The residuals (see Fig. S2 in the supporting information) indicate that an acceptable fit has been found. The lifetimes extracted for the two decay components are $\tau_1 = 50 \pm 60$ fs, and $\tau_2 = 600 \pm 170$ fs; corresponding

exponential decay functions are shown as coloured lines on Fig. 2e. Fig. 2d, show the spectral profile of the two DAS, k_1 and k_2: k_1 is a broad peak from ~1 eV < *eKE* < 3.1 eV, and is predominately negative for < 1 eV; while k_2 takes the form of a continually decreasing slope from 0 eV < *eKE* < 2.2 eV. The k_1 high energy cutoff of 3.1 eV agrees well with the adiabatic detachment energy for the nucleobase within $dGMP^-$, which was found to be 4.65 eV.[28] The negative intensity of k_1 < 1 eV is indicative of a population transfer from the higher *eKE* region to the lower *eKE* region. Note that the extracted τ_1 lifetime is within our temporal resolution.

Comparing the lifetimes obtained here (50 fs and 600 fs) with those for solvated $dGMP^-$ (120 fs and 680 fs) reveals a striking similarity: the two agree within error despite the radically different environments.[16] This strongly suggests that a similar decay pathway is occurring in both environments, despite the strong effect of the solvent on the energy of the $^1n\pi^*$ state.[65, 68] Analogous to $dAMP^-$,[26] our data suggests that the dynamics in $dGMP^-$ are occurring predominately on the ^1L_a excited state, with the $^1n\pi^*$ state not actively participating. This is in agreement with some theoretical predictions.[57, 61, 62]

Based on the above observations, we assign the initial motion observed in the time resolved photoelectron spectrum to relaxation of the excited system away from the Franck-Condon geometry, and the slower decay to internal conversion using a ^2E CI. If this assignment is correct, then by extension we propose that the previous biexponential kinetics observed in isolated Gua also correspond to dynamics solely upon a single excited state,[9] and excited state dynamics of the purine nucleobases may follow a similar mechanism. The DAS can then be correlated to the photodetachment spectra of different regions along the ^1L_a decay coordinate.

$dTMP^-$

The photophysics of Thy are of particular interest as photoinitiated cyclo-addition between two Thy groups is a leading form of DNA damage.[69] A number of experimental studies have focused on the decay dynamics of isolated Thy, when excited at 4.7 eV (266 nm). The dominant conformer in molecular beams is the biological keto tautomer.[70, 71] TR-IY experiments using multiphoton probes showed that isolated Thy has a much longer lived excited state than the other nucleobases; three decay constants could be associated with the relaxation, with lifetimes of approximately 100 fs and 5 ps for the first two decays.[9, 10, 72] The third feature has a lifetime of 2.8 ns, and has been assigned to intersystem crossing onto the $^3\pi\pi^*$ state, by measurement of the vibrational spectrum of the transient species.[72] TRPES, using a 4.96 eV (250 nm) pump and a 6.20 eV (200 nm) probe, were fit using three time constants of < 50, 530 and 6400 fs.[5] Presumably owing to the differing photoexcitation and single-photon ionisation energies, the TRPES data are not in perfect agreement with the TR-IY data. Nevertheless, a pattern for the early dynamics in which an ultrafast decay, followed by a decay of ~5 ps, emerges.

Numerous computational studies have been performed in an attempt to disentangle the initial dynamics of Thy. In the vertical excitation region, the S_1 is an optically dark state of $^1n\pi^*$ character, whilst the S_2 is the optically bright $^1\pi\pi^*$ state.[73] CIs have been located between the $^1\pi\pi^*$ and both $^1n\pi^*$ and S_0 states: the former has a boat conformation, puckered at C^6 and C^3, while the latter is puckered at the C^5 atom (see Fig. 3a for atom labels).[64, 73-77] From these computational studies, a number of possible explanations for the dynamics of Thy have emerged. Domcke and coworkers[74] calculated a barrierless reaction path to the $^1\pi\pi^*/S_0$ CI from the vertical Franck-Condon region, responsible for the fast time constant, whilst the slower time constant was assigned to trapping of excited state flux on the optically dark $^1n\pi^*$ state. On the other hand, Merchan *et al.* attributed the slower dynamics to trapping on the $^1\pi\pi^*$ state, without active contribution from the $^1n\pi^*$ state.[76] Interpretation of the time resolved photoelectron spectra, using the *ab initio* multi spawning (AIMS) technique, concluded that the initial femtosecond component results primarily from motion on the $^1\pi\pi^*$ state, without any change of electronic character.[11] The slower component was then suggested to be borne mainly from a barrier crossing at the $^1\pi\pi^*(S_2)/^1n\pi^*(S_1)$ CI. A key observation, however, was that multiple CI pathways are available, rather than just a single decay mechanism.

In the solution phase, Hare *et al.* found that a wavepacket bifurcation occurs in excited Thy, which may decay via two mechanisms.[2, 78] The excited state population mostly (~90%) undergoes direct relaxation via a $^1\pi\pi^*/S_0$ CI with sub-picosecond timescales,[1, 17-19] while the remaining population becomes trapped on the $^1n\pi^*$ state for 30 ps. They found that solvated dTMP displayed similar early time dynamics, but the slow component has a lifetime of 127 ps, indicating a much larger barrier to deactivation of the $^1n\pi^*$ state after ribosyl substitution. Similar to the purine bases, solvation destabilizes the $^1n\pi^*$ state significantly more than the $^1\pi\pi^*$ state, so comparisons between gas and solution phases may not be valid in mechanisms where the $^1n\pi^*$ state plays a role.

We have measured the dynamics of isolated $dTMP^-$, using TRPES following excitation at 4.66 eV. Fig. 3b and c shows the resultant background subtracted data and global fit, respectively. Unlike the purine nucleotides, two decay components are not adequate to fit the data: close inspection of Fig. 3e shows a small offset from the baseline at long time delays. The global fit was thus performed with three decay components, with the lifetime of the third component arbitrarily set to τ_3 = 5 ps. The data are reminiscent of those for the purine nucleobases, with a τ_2 = 211 ± 127 fs feature decreasing from 0 *eKE*, but remaining universally positive, and a faster τ_1 = 58 ± 111 fs feature that is positive around 1.5 eV, but negative for *eKE* < 1 eV. The significantly larger errors extracted for $dTMP^-$ compared to $dGMP^-$ are a consequence of the additional timescale required in the fit, reducing the steepness of χ^2 in phase space. Inspection of both Fig. 3b and Fig. S3 in the supporting information show the higher energy feature shifting to lower *eKE* as a function of time, a clear indication of sequential dynamics. The DAS for the picosecond component,

k_3, is mainly located at low *eKE*. However, the feature is too weak to make any definitive comments about its shape. A strong two-photon feature is observed for *eKE* > 2.1 eV, which is the adiabatic cut off for a one-photon probe. The appearance of the two-photon feature effectively extends the available probing window, although we note that convolution of the one- and two-photon probe peaks may complicate the data analysis. The initial rapid shift in *eKE* is especially visible in the two-photon signal.

The DAS of the τ_1 fs component (k_1) has considerable negative amplitude at *eKE* < 1 eV, and in fact the total integral of it is negative (see Fig. 3e). The overall negative integral indicates that we are observing population flowing from a region that has a lower ionisation cross-section into a region where the cross-section has increased. The two-photon feature for k_1 also shows a significant negative component. The large amount of negative signal in this feature is indicative of considerable population flow in the system; in the 2D spectra, this flow is clearly manifested as a shift to later onset time for the *eKE* < 1 eV feature and the two-photon feature, as can also be seen in Fig. S3 in the supporting information.

A direct comparison of the deprotonated nucleotide and isolated nucleobase dynamics does not appear to be possible, although some similarities are observed. By analogy with the purine nucleotides, as well as with reference to the sizable body of work describing the potential energy surfaces of Thy,[73-75, 77, 79] the initial τ_1 = 60 fs time constant can likely be assigned to motion of the wavepacket on the S_2 $^1\pi\pi^*$ state, from the vertical Franck-Condon region towards some local minimum. Assignment of the two slower features is less straightforward, and we shall use the identity of the long lived component, τ_3, to guide this discussion. As this feature manifests as a flat offset on the timescale of our experiment, of too small intensity to accurately fit, we can only assign it a lifetime ≥ 5 ps, which could in principle stretch into the nanosecond regime. If this feature is indeed very long lived (nanoseconds), then it is likely a triplet feature, as seen in neutral Thy.[72] The spectrum of k_3 should in principle aid with this assignment – the detachment energy of the triplet state can be calculated, and compared with the experimental spectrum. Even without direct spectral knowledge of k_3, calculations should be able to inform as to whether or not detachment from the triplet state is energetically feasible. If the τ_3 decay is associated with the triplet state decay, then presumably the 210 fs component corresponds to ground state relaxation via a $^1\pi\pi^*/S_0$ CI. In this scenario, the $^1n\pi^*$ state does not appear to play an active role, and we must presume that the picosecond channel observed in both isolated Thy and solvated dTMP has been quenched by either the presence of the charge or the unique geometry of the nucleotide. This scenario is shown schematically in Fig. 4a.

A second possible assignment of τ_3 is to the internal conversion from the $^1n\pi^*$ state. In this scenario, the lifetime is likely to be on the order of picoseconds, as in neutral Thy. The τ_2 = 210 fs component would then correspond to $^1\pi\pi^* \rightarrow {}^1n\pi^*$ internal conversion. Fig. 4b outlines this relaxation scheme. It is important to note that the 60 fs τ_1 component has negligible

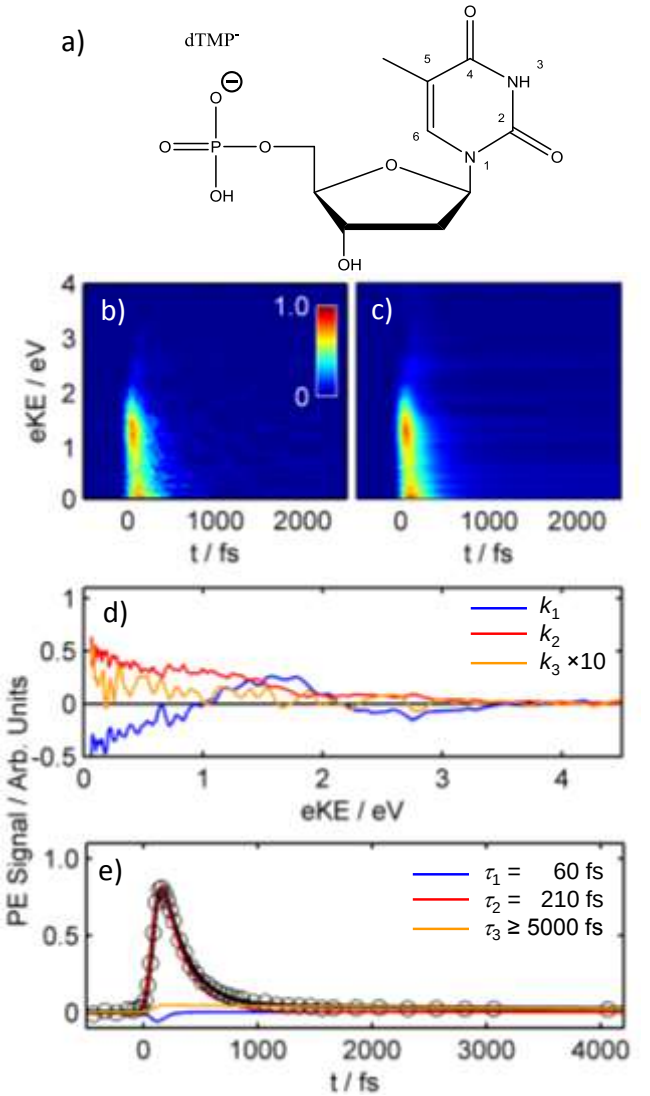

Fig. 3 a) Structure of $dTMP^-$; b) TRPES data from $dTMP^-$, presented as a false-colour plot; c) global fit to the TRPES data, using three exponential decay functions (one of which was arbitrarily set to 5 ps); d) decay associated spectra showing the spectra of the two fit components used to produce the fit. The long lived component, k_3, has been expanded ten-fold for clarity. e) integrated photoelectron signal as a function of delay time. Open circles give experimental data, coloured lines give the three exponential decay functions, and black line gives the total fitted integral.

absolute amplitude, and would be difficult to detect in non-differential measurements such as ion yield experiments.[9, 10] In these, only the 210 fs τ_2 component would then be observed. However, this lifetime is longer than that observed in experiments on neutral Thy (~100 fs), although variations in the potential landscape due the addition of the sugar/phosphate backbone and differences in initial temperature may well account for this. Note that in our experiments, the internal temperature is on the order of 300 K, whereas in a molecular beam, this is much lower: typically on the order of 10s K. The very small amplitude of k_3 appears to disagree with this model. But, our spectral window is limited, and the 3.1 eV probe may be too low for the majority of detachment from the $^1n\pi^*$. If this

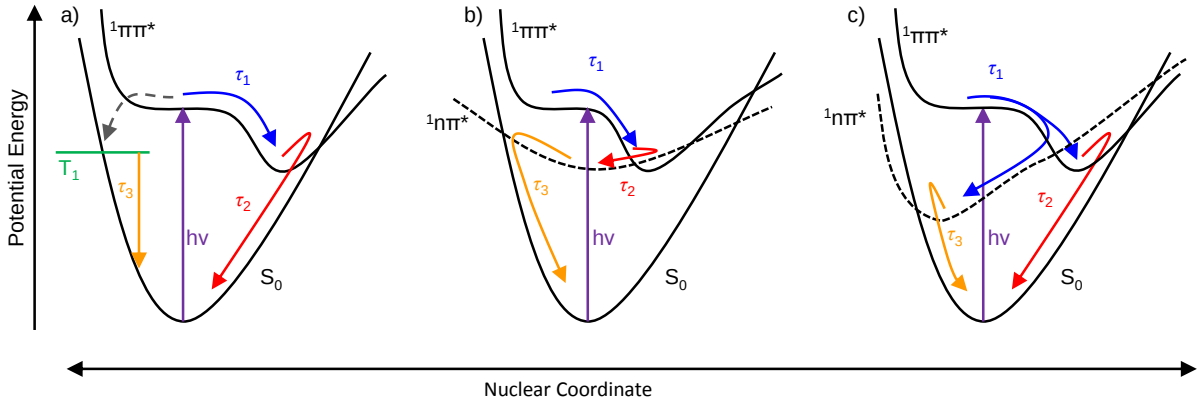

Fig. 4 Three possible mechanisms to describe the dynamics observed in $dTMP^-$. a) The two fast components correspond to motion upon the $^1\pi\pi^*$ state, followed by internal conversion, akin to $dGMP^-$. The long lived state is the result of intersystem crossing to a triplet state. b) The two fast time constants correspond to motion on the $^1\pi\pi^*$ state, followed by conversion to the $^1n\pi^*$ state, and the slow time constant is relaxation of the $^1n\pi^*$ state. c) The majority of population proceeds via a $^1\pi\pi^* \rightarrow S_0$ route, whilst a small portion becomes trapped upon the $^1n\pi^*$ state.

was case, a long lived component should be visible from two-photon detachment. No significant amplitude is seen in the DAS of the long lived component at *eKE* > 2.1 eV, although it may simply be the case that detachment signal from the $^1n\pi^*$ state is very weak due to a small cross section.

Finally, it is feasible that τ_3 is due to bifurcated population trapped on the $^1n\pi^*$ state, as has been observed in solution,[78] and suggested by photoelectron spectroscopy and *ab initio* calculations on Thy.[11] Fig. 4c gives a sketch of this mechanism. In this scenario, the remaining dynamics are likely similar to those described for the triplet scenario, with τ_1 being associated with rapid initial motion, and τ_2 with internal conversion from the $^1\pi\pi^*$ state to the ground state. We note that solvation significantly destabilizes the $^1n\pi^*$ state (as in the purine bases), and hence this mechanism is likely perturbed strongly in the gas phase.[71, 77] The short term dynamics are otherwise rather comparable with those in solution, perhaps again indicating a less active role of the $^1n\pi^*$ state than previously thought.

The above comparisons have all been between $dTMP^-$ and neutral Thy, and hence one may query whether substitution at the N^1 site has a great effect on the dynamics. The ion yield experiments of Brutschy and co-workers showed that almost identical dynamics are obtained for Thy and 1-methylthymine,[72] suggesting that the hydrogenated nucleobase is an acceptable model for the dynamics of Thy in more complex environments, however as this was a non-differential measurement, there may be additional masked features. Overall, it appears that although the specifics of the relaxation mechanism for $dTMP^-$ are debatable, our results represent important new information to which theoretical models can be benchmarked. Specifically, the spectral shape of the DAS should provide a basis for assigning the decay components to specific process by comparison with calculated time-resolved photoelectron spectra.

$dCMP^-$

The dynamics of cytosine (Cyt) in the gas phase have, until recently, been poorly understood. Early femtosecond experiments, using either TR-IY[9, 10] or TRPES[5] showed poor agreement. The ion yield experiments, performed with a 4.7 eV pump, gave biexponential decay kinetics with a fast component limited by the instrument response, and a slower component with a lifetime of 1.9 – 3.2 ps.[9, 10] The TRPES, performed with a 4.96 eV (250 nm) pump, resulted in triexponential kinetics, with lifetimes of <50 fs, 820 fs and 3.2 ps (the latter lifetime fixed to the TR-IY results by Kang *et al.*).[5]

The origin of this confusion is almost certainly due to multiple tautomers present in the molecular beam. Microwave[80] and high resolution IR[81, 82] spectroscopies reveal that there are (at least) three tautomers of Cyt present within a molecular beam. These are the biological keto tautomer, and the non-biological enol and imino tautomers, which are present in a ratio of approximately 4:4:1, respectively (from microwave experiments).[80] In nucleotides, the sugar/phosphate backbone is attached on the N^1 site, and hence the enol tautomer is unavailable in biological systems, whilst the imino tautomer interferes with base pairing, and so the primary biological tautomer is the keto form.[83]

Three recent experimental publications have sought to untangle the dynamics within Cyt to isolate the behaviour of each tautomer, and in particular to ascertain the nonadiabatic relaxation of the keto tautomer. Kosma *et al.* noted that the onset of absorption to the S_1 of the enol and imino tautomers is energetically higher than in the keto tautomer:[84] the keto-Cyt onset is ~3.90 eV (318 nm), whilst the enol-Cyt origin is ~4.46 eV (278 nm).[85, 86] Thus, by restricting pump wavelengths to $\lambda \geq$ 280 nm, these authors could selectively observe only dynamics of the keto-Cyt tautomer. Dynamics were tracked using TR-IY, pumped using either 4.28 or 4.43 eV (290 or 280 nm) radiation, and probed using 3 photons at 1.55 eV (800 nm). Three components were observed in the decay, with lifetimes of <100 fs, 1.1 (1.2) ps and >150 (55) ps for excitation with 4.28 (4.43) eV. The proposed assignment was ultrafast motion away from

the Franck-Condon region following photoexcitation to the $^1\pi\pi^*$ state, followed by internal conversion directly to the ground state. The long lived component was tentatively assigned to an excited state tautomerization;[84] recent theory has shown this to be feasible.[87]

Ho *et al*. used chemical substitution to measure tautomer-specific behaviour:[12] methylation at the C^1 position (where the ribose group attaches, see Fig. 5a) blocks keto-enol tautomerization, and also better represents the biological nucleotide. TR-IY experiments on Cyt-1Me with a range of pump energies, 4.13 eV ≤ $h\nu$ ≤ 4.77 eV (260 nm ≤ λ ≤ 300 nm), and a 1.55 eV probe, gave biexponential decay kinetics composed of an initial spike limited by the instrument response,

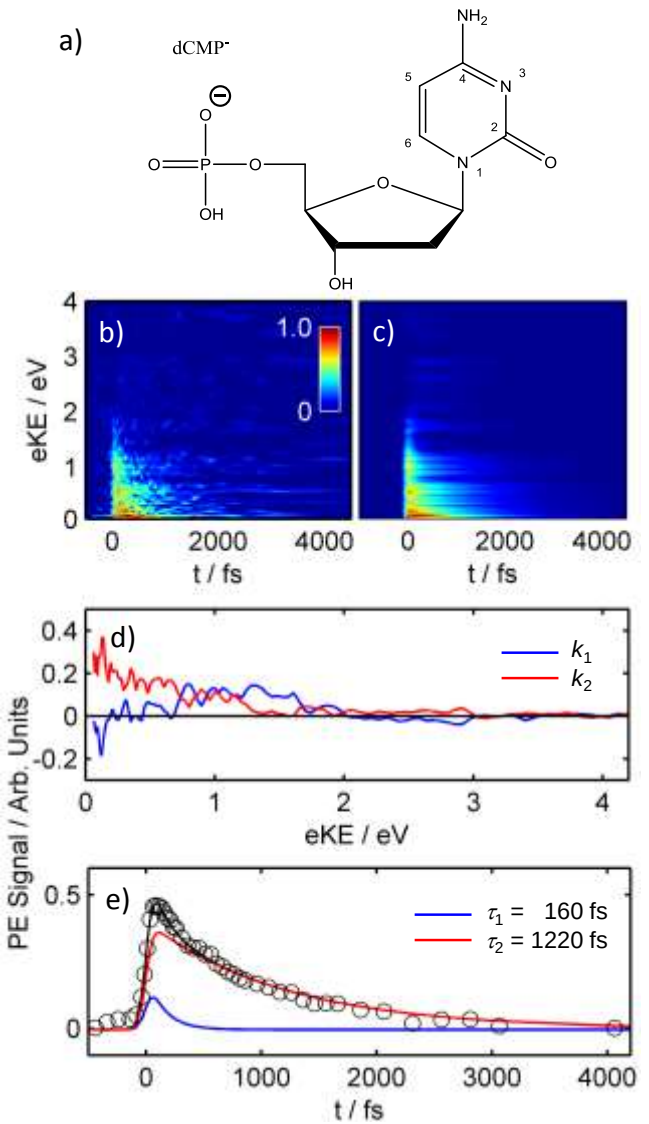

Fig. 5 a) Structure of $dCMP^-$; b) TRPES data from $dCMP^-$, presented as a false-colour plot; c) global fit to the TRPES data, using two exponential decay functions; d) decay associated spectra showing the spectra of the two fit components used to produce the fit; and e) integrated photoelectron signal as a function of delay time. Open circles give experimental data, coloured lines give the two exponential decay functions, and black line gives the total fitted integral.

and a decay with a lifetime of 0.4 - 1.3 ps (with shorter lifetimes at higher pump energies). Intriguingly, when pumped at 4.00 eV, the lifetime increases to 3.2 ps. The authors did not observe a slower component, and assigned the slower component observed by Kosma *et al.* to dynamics of fragments. Power dependency studies showed the initial spike to be primarily multi-photon in nature, although a one-photon component could not be ruled out.[12]

Very recently, Lobsiger *et al*. have measured linewidths in resonance-enhanced multiphoton ionisation experiments in order to determine the lifetime of keto-Cyt near the S_1 origin and shed light on the femtosecond measurements.[13] It was found that the lifetime of Cyt is *not* ultrafast at the absorption onset, and rapid dynamics only appear after ~500 cm^{-1} (60 meV) of excess energy is imparted in the S_1 state. The predominant vibrational progression was in an out-of-plane mode, and this was taken as evidence that relaxation occurs via a non-planar CI, as long as there is sufficient energy to access it.

Theoretical studies have gone a considerable way towards understanding the nonadiabatic dynamics of keto-Cyt. It is generally agreed that the S_1 state is of $^1\pi\pi^*$ character in the Franck-Condon region. The next two excited states are of $^1n\pi^*$ character, with the non-bonding orbital residing on either the N^3 ($^1n_N\pi^*$) or the O ($^1n_O\pi^*$) atom.[88-90] Several CIs with the ground state have been located, the three most accessible being a $^1\pi\pi^*/S_0$ CI from puckering on the C^6 atom, a $^1n_N\pi^*/S_0$ CI from puckering at the N^3 atom, or a semiplanar $^1n_O\pi^*/S_0$ CI.[64, 76, 88-93] Computations utilizing either minimum energy paths or surface hopping techniques have disagreed as to whether it is the C^6 pucker[76, 89] or the semiplanar[94, 95] CI which dominates, however very recently high level calculations have suggested that the $^1\pi\pi^*/S_0$ CI is the primary relaxation route, and that earlier calculations over-emphasized the importance of the $^1n_O\pi^*$ state.[88] This result is also supported by calculations on 5-fluorocytosine, which prevents facile state switching to the $^1n\pi^*$ states.[96, 97] A mechanism utilizing a puckered CI accords well with the findings that vibrational energy in out-of-plane modes is required before rapid relaxation can occur.[13]

In the solution phase, the dynamics of Cyt and CMP (the RNA nucleotide of Cyt) when excited at 4.66 eV are very much reminiscent of those of Thy and dTMP.[2, 78] Bifurcation of the population occurs between the optically bright $^1\pi\pi^*$ state and a dark state, presumably of $^1n\pi^*$ character. The dynamics of the rapid component are sub-picosecond,[1, 17-19] whilst the slow, dark, component decays in 12 ps.[78] As with Thy, moving to the nucleotide results in an increase in dark state lifetime, in this case to 34 ps, which indicates an increased barrier to relaxation. The dark state yield in CMP is considerably higher than in Cyt, at 41% and 9%, respectively,[78] perhaps indicative of a decrease in rate of decay purely upon the $^1\pi\pi^*$ state, and a change in dynamics upon building up to the nucleotide.

Fig. 5 shows the time-resolved photoelectron spectra and resultant global fit with two components for the isolated $dCMP^-$ anion. As above, a 4.66 eV pump and 3.10 eV probe was employed, and one colour backgrounds were subtracted. As

indicated by the larger residuals (see Fig. S2 in the supporting information), the signal to noise ratio for $dCMP^-$ is worse than for $dAMP^-$, $dGMP^-$ and $dTMP^-$. This is partly because the ion signal of $dCMP^-$ was lower compared to the others, presumably because it does not electrospray as easily, and partly due to reduced absorption and ionization cross sections. As with the purine nucleobases, one decay component in our kinetic fit is insufficient to capture the dynamics, and so a biexponential model has been used. Unlike $dTMP^-$, there is no long-time offset, although the relatively poorer signal-to-noise may obscure its presence. The two decay components have lifetimes of τ_1 = 160 fs and τ_2 = 1.22 ps, and the DAS spectral profile resembles the other nucleotides, with the fast component found at higher *eKE*, and the slower decay increasing towards *eKE* = 0, although no evidence of sequential dynamics (negative DAS) is observed. We have not assigned confidence intervals to the lifetimes extracted for $dCMP^-$, because the support plane analysis revealed that the χ^2 landscape of the fit is exceedingly shallow (see Fig. S1 in the supporting information) and so we cannot make any precise judgements of the errors. The poorer quality of these data mean they are somewhat less reliable than for the other nucleotides, and so conclusions drawn from them are by necessity more tenuous. We can only definitively state that $dCMP^-$ is considerably longer lived than the other nucleotides, but also that it shares similar DAS. Nonetheless, these measurements provide important benchmark data for theoretical simulations of $dCMP^-$ relaxation mechanisms.

$dCMP^-$ is remarkable in that it is the only nucleotide which possesses a significant component with a lifetime >1 ps. In particular, it is the only example where the hot nucleotide has longer lived dynamics than the isolated, cold nucleobase; Cyt-1Me has a lifetime of 0.5 ps when pumped at 4.59 eV.[12] There are two basic explanations for the increased lifetime of $dCMP^-$ compared to Cyt-1Me. Firstly, the general mechanism may be the same, relaxation mediated by the $^1\pi\pi^*/S_0$ CI, but the nucleotide may not reach the CI as easily as the methylated nucleobase. The CI geometry is thought to involve a puckering of the ring at the C^6 atom, [64, 76, 88-93] and it may be that inclusion of the sugar and phosphate impedes the required out of plane motion. In this scenario, all observed dynamics are borne from the $^1\pi\pi^*$ state, and the explanation follows that of the other nucleobases, with initial motion from the Franck-Condon region, followed by slower relaxation via the CI. The DAS appear to support such a mechanism, as they are qualitatively very similar to those of the other three nucleotides.

Alternatively, the mechanism for relaxation of $dCMP^-$ and Cyt-1Me need not be the same. The large difference in $^1n\pi^*$ utilization between Cyt and CMP in solution suggests that a significant modification to the electronic landscape of the chromophore may occur upon addition of the backbone.[78] Involvement of either of the $^1n\pi^*$ states cannot be ruled out. In fact, one could surmise that a bifurcation occurs, and that the two relaxation lifetimes reflect a split between relaxation using the $^1\pi\pi^*$ and $^1n\pi^*$ states. The lack of observed negative DAS tenuously supports this hypothesis.

Going forward, $dCMP^-$ perhaps presents the greatest mystery of the nucleotides studied. It is the only nucleotide which shows dynamics slower than the corresponding isolated nucleobase, tentatively suggesting a change in relaxation mechanics as the system is built up. Future improvements to the instrument should improve the signal-to-noise observed in the dispersed spectra, so that $dCMP^-$ can be studied more robustly, and a more concrete result obtained.

Comparison of Nucleotide Relaxation Mechanisms

One of the most striking aspects of the $dGMP^-$ data presented here is the similarity to those obtained previously for $dAMP^-$.[26] The shapes of the DAS for both the fast and slow components are extremely similar, although the fast feature in $dAMP^-$ has a positive component around half the width of that in $dGMP^-$, and extends to a lower *eKE* (~ 2.1 eV compared to ~ 3.1 eV). The first observation is perhaps a reflection of a flatter potential energy surface in the Franck Condon region for $dGMP^-$. The lower *eKE* cut-off is simply a reflection of the lower adiabatic binding energy of the nucleobase in $dGMP^-$ compared to $dAMP^-$ (4.65 eV *vs.* 5.65 eV), which is partly due to the configuration of the nucleotide, and partly due to an innately low binding energy in Gua.[28, 98] In the temporal domain, the lifetime of $dGMP^-$ is around twice as long than for $dAMP^-$, although still ultrafast. Given the similarities of the global fits, it seems probable that both $dAMP^-$ and $dGMP^-$ follow a similar relaxation mechanism. The agreement of $dGMP^-$ dynamics with solution phase experiments, as well as our previous work on $dAMP^-$, suggest that this mechanism follows a pathway involving only one electronic state, with no explicit internal conversion to a $^1n\pi^*$ state. Precise mechanistic details will of course differ, as the differing excited state lifetimes indicate, however, to a first approximation, a unified mechanism for relaxation of purine nucleotides seems feasible. Moreover, it appears that a solvent environment has a relatively small impact on the dynamics of the purine nucleotides. This makes our current findings particularly relevant as they can be directly compared to solution-phase work. In the DNA polymer however, the environment does cause major changes, in particular for Ade, where base-stacking leads to the formation of excimer states that are much longer lived.[1, 2, 21] Nevertheless, the direct internal conversion mechanism for $dAMP^-$ and $dGMP^-$ remains active even in the much larger systems and is the primary mechanism for transferring electronic energy into harmless heat.[2, 21, 99]

For the pyrimidine nucleotides, $dTMP^-$ and $dCMP^-$, less agreement in the excited state dynamics is observed. They both appear to follow a similar structure of rapid dynamics at higher *eKE*, followed by a slower decay in the lower *eKE* region. $dTMP^-$ employs definite sequential dynamics, while for $dCMP^-$ this is less definitive. Looking at the $dCMP^-$ time resolved spectra, normalized by each *eKE* slice (Fig. S3 in the supporting information), a small motion of maximum intensity towards later delays appears to be visible. This suggests that perhaps $dCMP^-$ also engages initially in rapid wavepacket motion, followed by exponential decay, as in the other

nucleotides. On the other hand, the longer lifetimes observed in $dCMP^-$ indicate that relaxation must be more hindered in this system. The excited state lifetime of $dCMP^-$ is approximately twice as long that of isolated Cyt-1Me,[12] suggesting that the presence of the sugar/phosphate backbone is very significant for the dynamics of this system. This is in opposition to the purine bases, where the dynamics seem to be solely driven by the nucleobase and are not affected by the backbone. $dTMP^-$ dynamics appear also to be mainly determined by the Thy nucleobase, but further work is required to assign the identity of the third component in the $dTMP^-$ dynamics. The spectral information provided through the DAS provides important information to aid in assigning the dynamics and, in combination with excited state calculations that consider the final states accessible through ionisation, a clearer picture of the potential energy surfaces and mechanisms may be generated. This is a prerequisite for studying processes that occur in the DNA polymer such as the photoinduced cyclo-addition of a pair of Thy nucleobases.[100]

Neutral-in-Anion Photoelectron Spectroscopy

A novel aspect of these experiments is that, although the overall nucleotide system is anionic, the phosphate group carries the excess charge and so the probed nucleobase moiety is essentially neutral. This "neutral-in-anion" scheme carries a number of interesting experimental features. The proximity of a charge to the nucleobase site lowers the electron binding energy, which means that longer wavelength lasers can be used to produce photoelectron spectra.[28] For time-resolved experiments, where very large datasets are required, background noise produced by deep UV lasers can be especially problematic, and so the possibility to use a near UV probe significantly enhances signal-to-noise. On the other hand, if background noise can be reduced, then using deep UV on a neutral-in-anion system allows for much deeper probing than in just the neutral alone. Caution must be applied to using a deep UV probe for nucleotides, however, as such a probe will produce a very large one-photon signal from detachment at the phosphate, which may mask the pump-probe signal. Additionally, such a probe would also be resonant with the excited states of the nucleobase. At 3.10 eV, there are no resonances, which makes the interpretation of the time-resolved spectra more straightforward.

In anion photoelectron spectroscopy, direct detachment to produce very low *eKE* electrons is inhibited by the Wigner threshold law.[101, 102] Essentially, the law states that due to the lack of Coulombic interactions between the outgoing electron and remaining neutral, a centrifugal barrier dominates the threshold behaviour. The upshot is that electrons with very low *eKE* are barely observed. In all the spectra presented here, strong signal is observed at $eKE = 0$, in apparent violation of the threshold law. This may be explained by the fact that the electron is detached from a region of the molecule that is spatially well separated from the excess electron on the phosphate. Hence, a cation is locally produced (and a zwitterion overall) for which the strong local Coulomb interactions may relax the Wigner laws for anions. Experiments are currently underway in our laboratory to quantify this effect.

In our experiments, we have assumed that the presence of a nearby charge does not significantly perturb the structure and dynamics of the nucleobase moiety. The similarities in dynamics in the purines between neutral nucleobases and anionic nucleotides suggest that this assumption may hold. On the other hand, each nucleotide has a unique gas phase conformation,[27] so the charge may not remain a spectator in all systems. Further theory is required to explore the effect of the charge on the dynamics and excited states. A second concern of the experimental scheme is that detachment leads to a zwitterionic final state, where an electron resides on the phosphate, and a hole is on the nucleobase. Resonance enhanced two-photon photodetachment showed that this zwitterion is only the lowest lying neutral state for $dGMP^-$,[28] and in the other nucleotides the neutral species without a charged phosphate is lower in energy. These considerations will have no effect on comparisons between nucleotides, as the same class of final state is accessed in all of them. Likewise, the nature of the final state should not affect dynamics comparisons between anions and neutral species, although different Franck-Condon factors may complicate detailed spectral comparisons.

Conclusions

Using combination of ESI mass spectrometry and TRPES, the relaxation dynamics of excited deprotonated nucleotides have been measured. For $dGMP^-$, this represents the first time TRPES has been applied to a gas-phase Gua moiety. The relaxation dynamics of $dGMP^-$ are analogous to those of $dAMP^-$, suggesting that both purine nucleotides relax in a similar manner with biexponential decay kinetics assigned to wavepacket motion on the $^1\pi\pi^*$ state followed by internal conversion on the $^1\pi\pi^*$ to the S_0 through a CI. $dTMP^-$ showed behaviour reminiscent of isolated Thy, though not identical. A long lived component was seen in the relaxation of Thy, in addition to two rapid components. Three feasible mechanisms were presented to interpret these dynamics of which rapid wavepacket motion on the $^1\pi\pi^*$ state, followed by internal conversion to the ground state is the most consistent with our data. The long lived component is probably due to population trapped in the $^1n\pi^*$ state, or possibly in a triplet state. Finally, $dCMP^-$ showed slower dynamics than the other nucleotides. For this the dynamics likely involve motion entirely on the $^1\pi\pi^*$ surface, as with the other nucleobases. Intriguingly, $dCMP^-$ is longer lived than isolated Cyt, suggesting that the presence of the sugar/phosphate backbone inhibits the system reaching an appropriate CI geometry.

These results present benchmark data for the dynamics of isolated nucleotides. Advances in *ab initio* techniques will allow complex simulations to be directly compared to experimental results, providing high levels of detail about the relaxation mechanisms. These results also present a first step towards understanding the dynamics of more complex isolated

DNA systems, such as oligonucleotides with stacked or paired bases, which can also be generated using ESI. Finally, our results show that a direct comparison between solution phase and gas phase experiments on these systems provides deeper insights by considering the effects solvation has on the location of excited states.

Acknowledgements

The project was funded by the Leverhulme Trust (F/00215/BH) and the EPSRC (EP/D073472/1). V.G.S. thanks the Royal Society for a University Research Fellowship. J.R.R.V. is grateful to the European Research Council for a Starting Grant (306536).

Notes and references

[a] Department of Chemistry, University of Durham, Durham DH1 3LE, United Kingdom
[b] Department of Chemistry, University of Warwick, Coventry CV4 7AL, United Kingdom.
† Present address: Ultrafast X-ray Science Laboratory, Chemical Sciences Division, Lawrence Berkeley National Laboratory, Berkeley, California 94720, United States

Electronic Supplementary Information (ESI) available: Residuals and confidence intervals of global fits; TRPES normalized by *eKE* slices. See DOI: 10.1039/b000000x/

1. C. E. Crespo-Hernández, B. Cohen, P. M. Hare and B. Kohler, *Chem. Rev.*, 2004, **104**, 1977-2020.
2. C. T. Middleton, K. de La Harpe, C. Su, Y. K. Law, C. E. Crespo-Hernández and B. Kohler, *Annu. Rev. Phys. Chem.*, 2009, **60**, 217-239.
3. K. Kleinermanns, D. Nachtigallová and M. S. de Vries, *Int. Rev. Phys. Chem.*, 2013, **32**, 308-342.
4. M. K. Shukla and J. Leszczynski, *J. Biomol. Struct. Dyn.*, 2007, **25**, 93-118.
5. S. Ullrich, T. Schultz, M. Z. Zgierski and A. Stolow, *Phys. Chem. Chem. Phys.*, 2004, **6**, 2796-2801.
6. H. Satzger, D. Townsend, M. Z. Zgierski, S. Patchkovskii, S. Ullrich and A. Stolow, *Proc. Nat. Acad. Sci. U.S.A.*, 2006, **103**, 10196-10201.
7. M. G. D. Nix, A. L. Devine, B. Cronin and M. N. R. Ashfold, *J. Chem. Phys.*, 2007, **126**, 124312.
8. K. L. Wells, D. J. Hadden, M. G. D. Nix and V. G. Stavros, *J. Phys. Chem. Lett.*, 2010, **1**, 993-996.
9. C. Canuel, M. Mons, F. Piuzzi, B. Tardivel, I. Dimicoli and M. Elhanine, *J. Chem. Phys.*, 2005, **122**, 074316.
10. H. Kang, K. T. Lee, B. Jung, Y. J. Ko and S. K. Kim, *J. Am. Chem. Soc.*, 2002, **124**, 12958-12959.
11. H. R. Hudock, B. G. Levine, A. L. Thompson, H. Satzger, D. Townsend, N. Gador, S. Ullrich, A. Stolow and T. J. Martínez, *J. Phys. Chem. A*, 2007, **111**, 8500-8508.
12. J.-W. Ho, H.-C. Yen, W.-K. Chou, C.-N. Weng, L.-H. Cheng, H.-Q. Shi, S.-H. Lai and P.-Y. Cheng, *J. Phys. Chem. A*, 2011, **115**, 8406-8418.
13. S. Lobsiger, M. A. Trachsel, H.-M. Frey and S. Leutwyler, *J. Phys. Chem. B*, 2013, **117**, 6106-6115.
14. D. Onidas, D. Markovitsi, S. Marguet, A. Sharonov and T. Gustavsson, *J. Phys. Chem. B*, 2002, **106**, 11367-11374.
15. T. Gustavsson, A. Sharonov, D. Onidas and D. Markovitsi, *Chem. Phys. Lett.*, 2002, **356**, 49-54.
16. M. C. Stuhldreier and F. Temps, *Faraday Discuss.*, 2013, **163**, 173-188.
17. J.-M. L. Pecourt, J. Peon and B. Kohler, *J. Am. Chem. Soc.*, 2000, **122**, 9348-9349.
18. J.-M. L. Pecourt, J. Peon and B. Kohler, *J. Am. Chem. Soc.*, 2001, **123**, 10370-10378.
19. J. Peon and A. H. Zewail, *Chem. Phys. Lett.*, 2001, **348**, 255-262.
20. B. Cohen, P. M. Hare and B. Kohler, *J. Am. Chem. Soc.*, 2003, **125**, 13594-13601.
21. C. E. Crespo-Hernandez, B. Cohen and B. Kohler, *Nature*, 2005, **436**, 1141-1144.
22. I. Buchvarov, Q. Wang, M. Raytchev, A. Trifonov and T. Fiebig, *Proc. Nat. Acad. Sci. U.S.A.*, 2007, **104**, 4794-4797.
23. T. Takaya, C. Su, K. de La Harpe, C. E. Crespo-Hernández and B. Kohler, *Proc. Nat. Acad. Sci. U.S.A.*, 2008, **105**, 10285-10290.
24. K. de La Harpe and B. Kohler, *J. Phys. Chem. Lett.*, 2011, **2**, 133-138.
25. I. Vayá, T. Gustavsson, T. Douki, Y. Berlin and D. Markovitsi, *J. Am. Chem. Soc.*, 2012, **134**, 11366-11368.
26. A. S. Chatterley, C. W. West, G. M. Roberts, V. G. Stavros and J. R. Verlet, *J. Phys. Chem. Lett.*, 2014, **5**, 843-848.
27. Y.-w. Nei, N. Hallowita, J. D. Steill, J. Oomens and M. T. Rodgers, *J. Phys. Chem. A*, 2013, **117**, 1319-1335.
28. A. S. Chatterley, A. S. Johns, V. G. Stavros and J. R. Verlet, *J. Phys. Chem. A*, 2013, **117**, 5299-5305.
29. C. Z. Bisgaard, H. Satzger, S. Ullrich and A. Stolow, *ChemPhysChem*, 2009, **10**, 101-110.
30. L. Blancafort, *J. Am. Chem. Soc.*, 2005, **128**, 210-219.
31. C. M. Marian, *J. Chem. Phys.*, 2005, **122**, 104314.
32. S. Perun, A. L. Sobolewski and W. Domcke, *J. Am. Chem. Soc.*, 2005, **127**, 6257-6265.
33. L. Serrano-Andrés, M. Merchán and A. C. Borin, *Chemistry – A European Journal*, 2006, **12**, 6559-6571.
34. L. Serrano-Andrés, M. Merchán and A. C. Borin, *Proc. Nat. Acad. Sci. U.S.A.*, 2006, **103**, 8691-8696.
35. M. Barbatti and H. Lischka, *J. Am. Chem. Soc.*, 2008, **130**, 6831-6839.
36. E. Fabiano and W. Thiel, *J. Phys. Chem. A*, 2008, **112**, 6859-6863.
37. I. Conti, M. Garavelli and G. Orlandi, *J. Am. Chem. Soc.*, 2009, **131**, 16108-16118.
38. Y. Lei, S. Yuan, Y. Dou, Y. Wang and Z. Wen, *J. Phys. Chem. A*, 2008, **112**, 8497-8504.
39. A. N. Alexandrova, J. C. Tully and G. Granucci, *J. Phys. Chem. B*, 2010, **114**, 12116-12128.
40. M. Barbatti, A. J. A. Aquino, J. J. Szymczak, D. Nachtigallová, P. Hobza and H. Lischka, *Proc. Nat. Acad. Sci. U.S.A.*, 2010, **107**, 21453-21458.
41. M. Barbatti, Z. Lan, R. Crespo-Otero, J. J. Szymczak, H. Lischka and W. Thiel, *J. Chem. Phys.*, 2012, **137**, 22A503-514.

42. J. A. Boeyens, *Journal of Crystal and Molecular Structure*, 1978, **8**, 317-320.
43. M. Smits, C. A. de Lange, S. Ullrich, T. Schultz, M. Schmitt, J. G. Underwood, J. P. Shaffer, D. M. Rayner and A. Stolow, *Rev. Sci. Instrum.*, 2003, **74**, 4812-4817.
44. D. A. Horke, G. M. Roberts, J. Lecointre and J. R. R. Verlet, *Rev. Sci. Instrum.*, 2012, **83**, 063101.
45. J. Lecointre, G. M. Roberts, D. A. Horke and J. R. R. Verlet, *J. Phys. Chem. A*, 2010, **114**, 11216-11224.
46. D. A. Horke and J. R. R. Verlet, *Phys. Chem. Chem. Phys.*, 2011, **13**, 19546-19552.
47. A. T. J. B. Eppink and D. H. Parker, *Rev. Sci. Instrum.*, 1997, **68**, 3477-3484.
48. G. M. Roberts, J. L. Nixon, J. Lecointre, E. Wrede and J. R. R. Verlet, *Rev. Sci. Instrum.*, 2009, **80**, 053104.
49. C. R. S. Mooney, D. A. Horke, A. S. Chatterley, A. Simperler, H. H. Fielding and J. R. R. Verlet, *Chem. Sci.*, 2013, **4**, 921-927.
50. P. Hockett, *Faraday Discuss.*, 2013, **163**, 513-543.
51. M. Staniforth and V. G. Stavros, *Proceedings of the Royal Society A: Mathematical, Physical and Engineering Science*, 2013, **469**, 20130458.
52. E. Nir, C. Janzen, P. Imhof, K. Kleinermanns and M. S. de Vries, *J. Chem. Phys.*, 2001, **115**, 4604-4611.
53. W. Chin, M. Mons, I. Dimicoli, F. Piuzzi, B. Tardivel and M. Elhanine, *Eur. Phys. J. D*, 2002, **20**, 347-355.
54. M. Mons, I. Dimicoli, F. Piuzzi, B. Tardivel and M. Elhanine, *J. Phys. Chem. A*, 2002, **106**, 5088-5094.
55. H. Langer and N. L. Doltsinis, *Phys. Chem. Chem. Phys.*, 2004, **6**, 2742-2748.
56. H. Langer, N. L. Doltsinis and D. Marx, *ChemPhysChem*, 2005, **6**, 1734-1737.
57. H. Chen and S. Li, *J. Chem. Phys.*, 2006, **124**, 154315.
58. C. M. Marian, *J. Phys. Chem. A*, 2007, **111**, 1545-1553.
59. L. Serrano-Andrés, M. Merchán and A. C. Borin, *J. Am. Chem. Soc.*, 2008, **130**, 2473-2484.
60. S. Yamazaki, W. Domcke and A. L. Sobolewski, *J. Phys. Chem. A*, 2008, **112**, 11965-11968.
61. Z. Lan, E. Fabiano and W. Thiel, *ChemPhysChem*, 2009, **10**, 1225-1229.
62. M. Barbatti, J. J. Szymczak, A. J. A. Aquino, D. Nachtigallova and H. Lischka, *J. Chem. Phys.*, 2011, **134**, 014304.
63. F. Santoro, R. Improta, T. Fahleson, J. Kauczor, P. Norman and S. Coriani, *J. Phys. Chem. Lett.*, 2014, **5**, 1806-1811.
64. L. Serrano-Andrés and M. Merchán, *J. Photochem. Photobiol. C*, 2009, **10**, 21-32.
65. M. Parac, M. Doerr, C. M. Marian and W. Thiel, *J. Comput. Chem.*, 2010, **31**, 90-106.
66. V. Karunakaran, K. Kleinermanns, R. Improta and S. A. Kovalenko, *J. Am. Chem. Soc.*, 2009, **131**, 5839-5850.
67. F.-A. Miannay, T. Gustavsson, A. Banyasz and D. Markovitsi, *J. Phys. Chem. A*, 2010, **114**, 3256-3263.
68. B. Heggen, Z. Lan and W. Thiel, *Phys. Chem. Chem. Phys.*, 2012, **14**, 8137-8146.
69. D. S. Goodsell, *The Oncologist*, 2001, **6**, 298-299.
70. B. B. Brady, L. A. Peteanu and D. H. Levy, *Chem. Phys. Lett.*, 1988, **147**, 538-543.
71. M. K. Shukla and J. Leszczynski, *Wiley Interdisciplinary Reviews: Computational Molecular Science*, 2013.
72. M. Kunitski, Y. Nosenko and B. Brutschy, *ChemPhysChem*, 2011, **12**, 2024-2030.
73. G. Zechmann and M. Barbatti, *J. Phys. Chem. A*, 2008, **112**, 8273-8279.
74. S. Perun, A. L. Sobolewski and W. Domcke, *J. Phys. Chem. A*, 2006, **110**, 13238-13244.
75. S. Yamazaki and T. Taketsugu, *J. Phys. Chem. A*, 2011, **116**, 491-503.
76. M. Merchán, R. González-Luque, T. Climent, L. Serrano-Andrés, E. Rodríguez, M. Reguero and D. Peláez, *J. Phys. Chem. B*, 2006, **110**, 26471-26476.
77. D. Picconi, V. Barone, A. Lami, F. Santoro and R. Improta, *ChemPhysChem*, 2011, **12**, 1957-1968.
78. P. M. Hare, C. E. Crespo-Hernández and B. Kohler, *Proc. Nat. Acad. Sci. U.S.A.*, 2007, **104**, 435-440.
79. J. Gonzalez-Vazquez, L. Gonzalez, E. Samoylova and T. Schultz, *Phys. Chem. Chem. Phys.*, 2009, **11**, 3927-3934.
80. R. D. Brown, P. D. Godfrey, D. McNaughton and A. P. Pierlot, *J. Am. Chem. Soc.*, 1989, **111**, 2308-2310.
81. M. Szczesniak, K. Szczepaniak, J. S. Kwiatkowski, K. KuBulat and W. B. Person, *J. Am. Chem. Soc.*, 1988, **110**, 8319-8330.
82. G. Bazso, G. Tarczay, G. Fogarasi and P. G. Szalay, *Phys. Chem. Chem. Phys.*, 2011, **13**, 6799-6807.
83. D. L. Barker and R. E. Marsh, *Acta Crystallographica*, 1964, **17**, 1581-1587.
84. K. Kosma, C. Schröter, E. Samoylova, I. V. Hertel and T. Schultz, *J. Am. Chem. Soc.*, 2009, **131**, 16939-16943.
85. E. Nir, I. Hunig, K. Kleinermanns and M. S. de Vries, *Phys. Chem. Chem. Phys.*, 2003, **5**, 4780-4785.
86. E. Nir, M. Müller, L. I. Grace and M. S. de Vries, *Chem. Phys. Lett.*, 2002, **355**, 59-64.
87. C. G. Triandafillou and S. Matsika, *J. Phys. Chem. A*, 2013, **117**, 12165-12174.
88. A. Nakayama, Y. Harabuchi, S. Yamazaki and T. Taketsugu, *Phys. Chem. Chem. Phys.*, 2013, **15**, 12322-12339.
89. M. Merchán and L. Serrano-Andrés, *J. Am. Chem. Soc.*, 2003, **125**, 8108-8109.
90. K. Tomić, J. Tatchen and C. M. Marian, *J. Phys. Chem. A*, 2005, **109**, 8410-8418.
91. K. A. Kistler and S. Matsika, *J. Chem. Phys.*, 2008, **128**, 215102-215114.
92. K. A. Kistler and S. Matsika, *J. Phys. Chem. A*, 2007, **111**, 2650-2661.
93. N. Ismail, L. Blancafort, M. Olivucci, B. Kohler and M. A. Robb, *J. Am. Chem. Soc.*, 2002, **124**, 6818-6819.
94. H. R. Hudock and T. J. Martínez, *ChemPhysChem*, 2008, **9**, 2486-2490.
95. M. Barbatti, A. J. A. Aquino, J. J. Szymczak, D. Nachtigallova and H. Lischka, *Phys. Chem. Chem. Phys.*, 2011, **13**, 6145-6155.
96. M. Z. Zgierski, S. Patchkovskii and E. C. Lim, *J. Chem. Phys.*, 2005, **123**, 081101.
97. M. Z. Zgierski, S. Patchkovskii, T. Fujiwara and E. C. Lim, *J. Phys. Chem. A*, 2005, **109**, 9384-9387.

98. X. Yang, X.-B. Wang, E. R. Vorpagel and L.-S. Wang, *Proc. Nat. Acad. Sci. U.S.A.*, 2004, **101**, 17588-17592.
99. B. Kohler, *J. Phys. Chem. Lett.*, 2010, **1**, 2047-2053.
100. W. J. Schreier, T. E. Schrader, F. O. Koller, P. Gilch, C. E. Crespo-Hernández, V. N. Swaminathan, T. Carell, W. Zinth and B. Kohler, *Science*, 2007, **315**, 625-629.
101. J. P. David, *Rep. Prog. Phys.*, 2004, **67**, 857-901.
102. E. P. Wigner, *Phys. Rev.*, 1948, **73**, 1002-1009.